OCEAN DIGEST

Quarterly Newsletter of the Ocean Society of India

Volume 4 | Issue 2 | Aug 2017 | ISSN 2394-1928

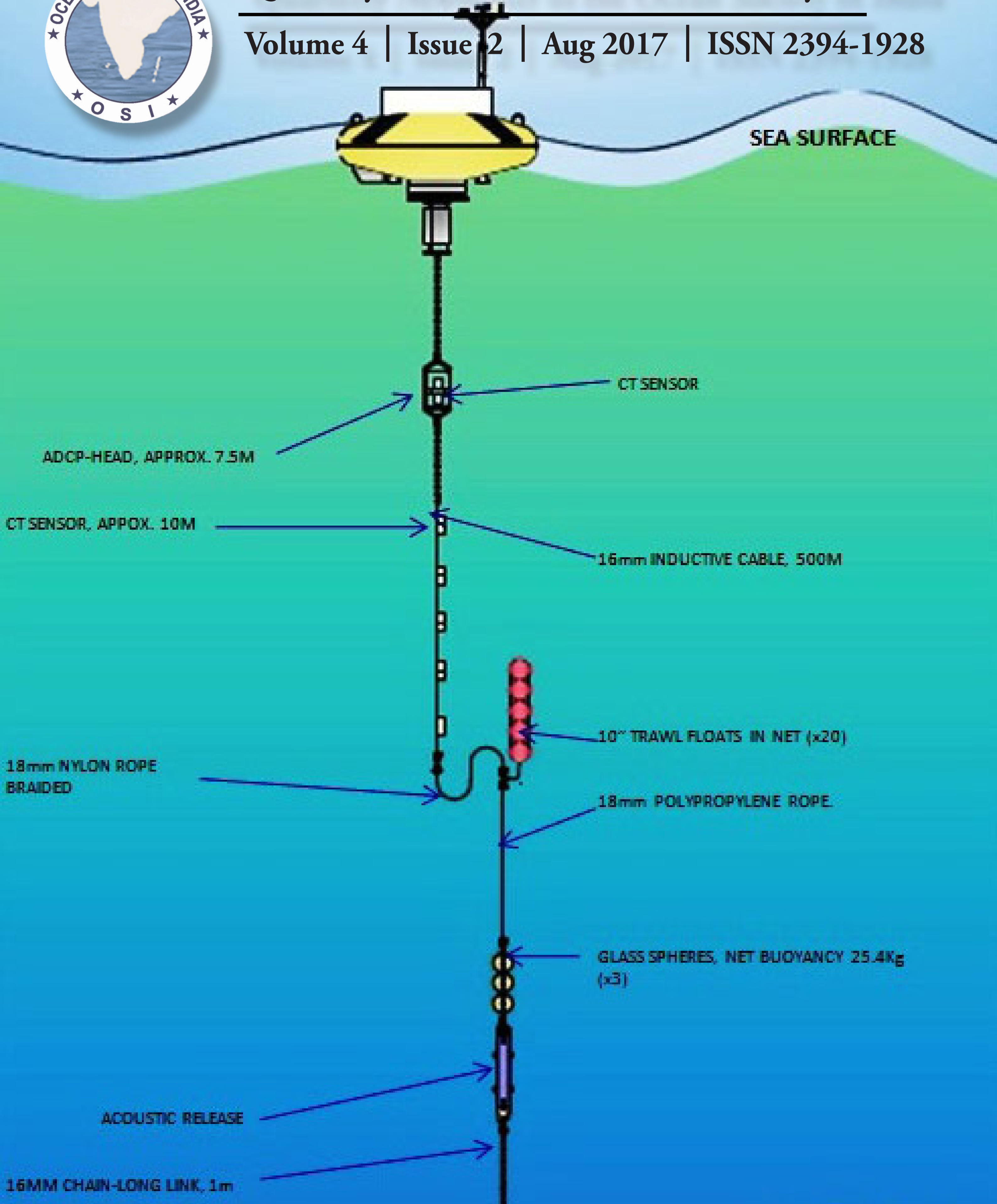

Wave measurements in high seas

Invited Article

R. Venkatesan and K. Jossia Joseph
National Institute of Ocean Technology, Chennai

1. Introduction

Ocean waves are critical for people who venture into the sea and play a significant role on air sea flux exchange and mixed layer dynamics. Apart from this, waves remain dominant factor of the design of coastal/offshore structures, shoreline stability, sailing notifications and port/harbour operations. The generation and propagation of wave depends on many atmospheric and oceanic processes and hence is a complex process. The climate change induced variability in wave characteristics has significant impact on coastal and shoreline dynamics.

The waves can be classified based on various criteria such as generating area, relative water depth and wave spectral characteristics. Based on generating area, waves are termed as sea waves, which are formed due to local winds and swell waves formed by the distant storms. The ratio between water depth (d) and wave length (L) is used to indicate deep water waves ($d/L>0.5$), intermediate water waves ($0.5>d/L>0.05$) and shallow water waves ($d/L<0.05$). The wave spectra in general exhibit single peaks, double peaks or multi-peaks, indicating the presence of waves arriving from various directions. Single peaked spectra indicate the dominance of sea or swell waves whereas the double peak and multi peaks indicate the presence of sea waves and swell waves. The waves are in general single peaked during southwest monsoon season in North Indian Ocean, pointing towards the significant contribution of southern ocean in modulating the North Indian Ocean wave climate.

The importance of waves on scientific as well as marine operations necessitates systematic measurement. The time series measurement for sufficiently long period is required for assessing the wave characteristics, which is essential for preliminary planning of various coastal structures. The systematic measurement of waves in North Indian Ocean initiated in 1997 with the inception of moored buoy network established under National Institute of Ocean Technology (NIOT), Chennai. At present Indian National Centre for Ocean Information Services (INCOIS), Hyderabad operates a wave rider buoy network along the coastal waters of India. The availability of satellite data and numerical models provides the spatial variability of waves. This has in general helped to identify the major characteristics of waves and its variability. The ocean wave forecast has advanced significantly in the recent decade, however remains tricky for the swell wave prediction. North Indian Ocean records significant contribution from swell waves and hence accurate prediction requires the simulation of swell wave part of the wave spectra. The validation of satellite measurements & model data and ocean state forecast greatly depends on the validity of the ground truth, since buoy measurements provide the sole source of ground truth.

2. Wave Measurement

The wave information is a decisive factor in sailing notifications and hence wave measurements were carried out routinely in ships. The visual observations were the first source of wave information, which were restricted to the ship track, mostly during fair weather conditions and were prone to human

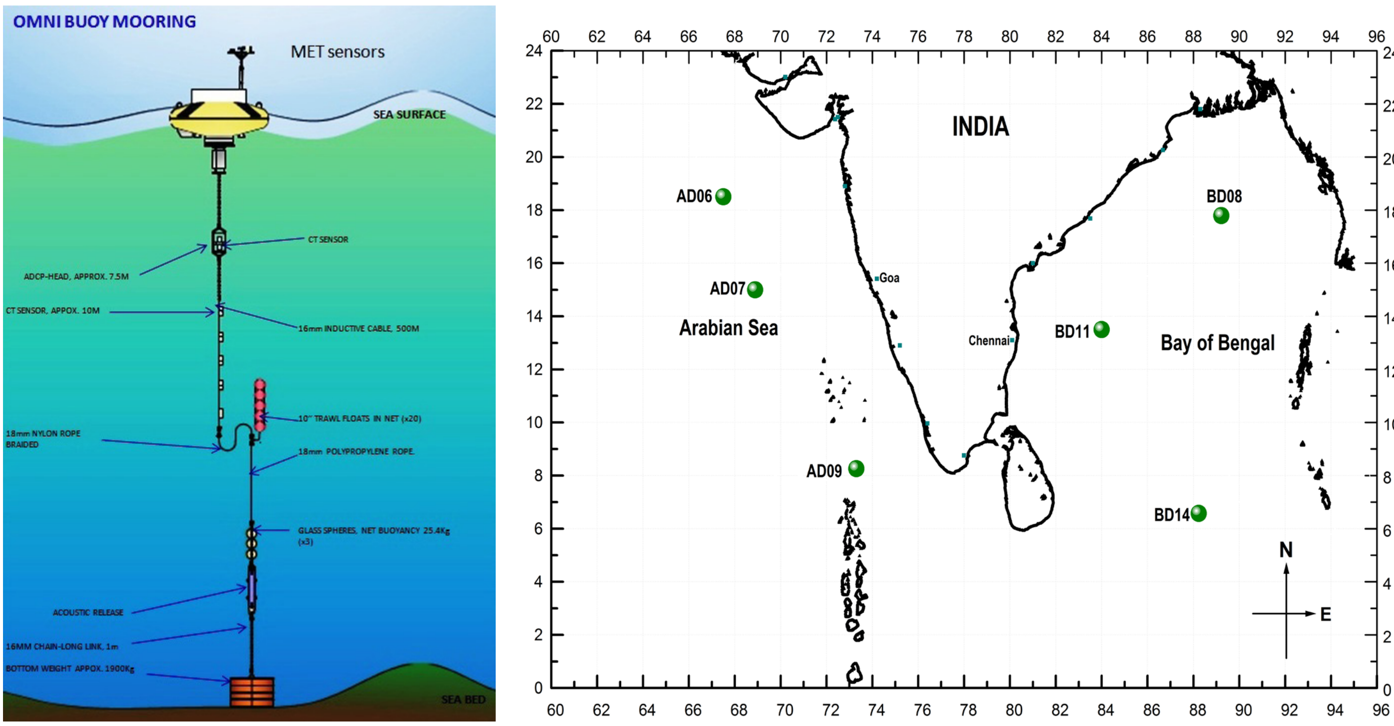

Figure 1: (a) Moored data buoy (b) Moored buoy network with deep sea wave measurement.

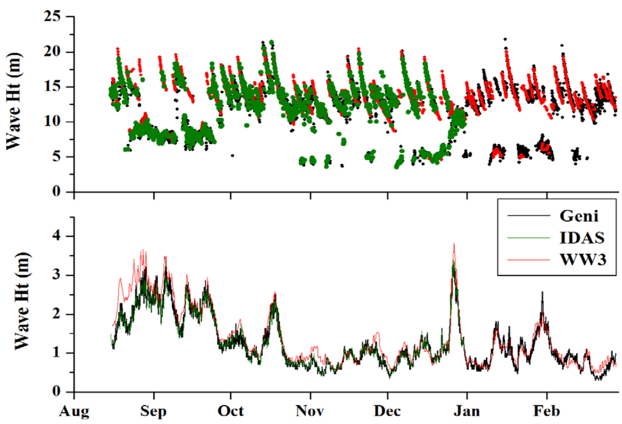

Figure 2: Comparison of buoys and model wave data.

error. The systematic measurement of waves started along with tide measurements in ports and harbour with installing a wave staff, but limited to wave height information. The invention of Directional Wave Rider (DWR) buoys paved the way for systematic wave measurements by providing spectral wave data including, sea and swell wave details.

Datawell Wave Rider Buoy measures vertical acceleration by means of an accelerometer. It consists of a spherical buoy designed to float on the sea surface and is moored to the seabed with special arrangement to maintain the free floating characteristics of the buoy. The wave elevation can then be obtained by twice integrating the acceleration. The horizontal acceleration is measured using two accelerometers and an onboard compass gives the directional displacement in two horizontal axes. The vertical displacement and wave slopes are utilized to compute the wave direction and other spectral wave parameters. The major disadvantage of DWR is the restriction of its use to only coastal waters.

The moored data buoys integrated with Seatex wave sensor MRU (Motion Reference Unit) evaded the limitations of DWR, with the feasibility to be deployed in coastal as well as deep ocean (Fig. 1). It is in this context moored instrumented buoys offer the most suitable and dependable platforms for uninterrupted data collection at selected locations during all types of weather throughout the year and for real time collection/ dissemination through satellite communication networks (Venkatesan et. al., 2013).

The wave sensor MRU is an inertial altitude heading reference system with dynamic linear motion measurement capability. The MRU outputs absolute Roll, Pitch along with Heading and relative heave in addition to acceleration, velocity of linear motions and angular velocity. The wave data is measured at a rate of 1 Hz for 17 minutes at every three hours. The processor on the buoy applies wave analysis software, which uses a Fast Fourier Transform on the wave record to obtain wave spectra. Both directional and non-directional analysis was carried out to calculate a range of wave parameters.

3. Development of wave processing software

Unlike the many oceanic parameters, the measurement of waves, specifically the directional wave measurement requires sophisticated instruments, measurement for comparatively longer period and dedicated processing unit to estimate the various components. The complex procedure

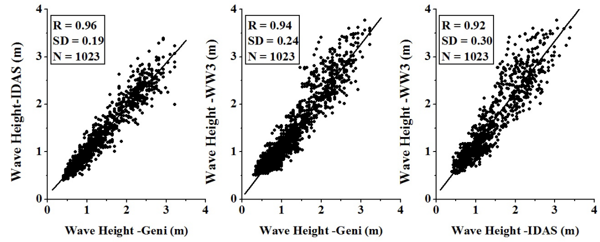

Figure 3: Scatter plots of significant wave height between buoys and satellite.

involved in directional wave measurements and the higher cost of maintenance of these instruments, restricted many organizations in venturing into this field. NIOT initiated directional wave measurements by integrating the Seatex MRU in the moored data buoys. The processing software was integrated with the buoy central processing unit GENI, which is provided by the Fugro Oceanor AS (Barstow and Krogstad, 1984; NDBC Technical Document, 1996). NIOT developed an indigenized data acquisition system (IDAS) for processing the sensor data as part of indigenization efforts. The indigenization of directional wave measurement was the most complex part and required extensive research, review and analysis.

The wave processing software was successfully developed for processing the wave sensor data (Heave, Pitch, Roll and Heading). The pitch and roll are converted to earth-fixed east-west and north-south wave slopes. Spectra and cross-spectral calculations are carried out using heave and wave slopes. Various spectral moments are obtained which are used for computing the spectral wave parameters

Moments of the spectrum (mk) = $\int_{0.04}^{0.5} f^k s(f)df$
where s(f) is the spectral density

Significant wave height (Hm0) = 4 * sqrt(m0)

Average wave period based on m0 and m2 (Tm02) = sqrt (m0/m2)

Mean wave direction (Mdir) = $\tan^{-1}$(b1/a1), where a1 and b1 are the directional Fourier coefficients.

In order to validate the software, a data buoy BD02 (Lat:

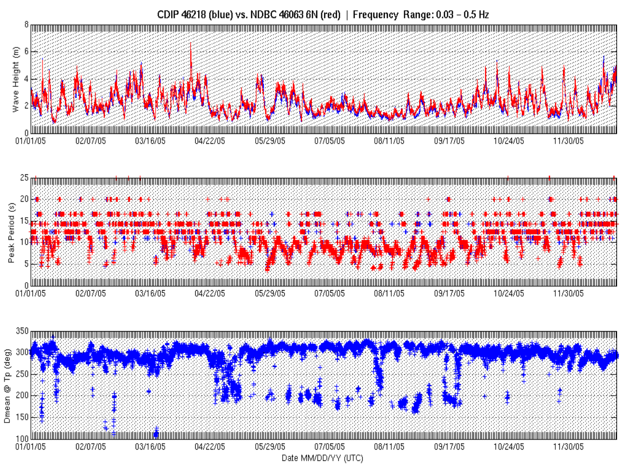

Figure 4: Inter-comparison of wave parameters CDIP vs. NDBC for PP-WET (top) - wave height, (middle) - peak wave period and (bottom) - wave direction @ peak period .

Figure 5: Datawell Wave Rider Buoy and the view of deployed buoys.

17.92N, Long: 89.72E) with indigenized wave software was deployed in Northern Bay off Paradip at a depth of 2300 m along with another buoy BD08 (18.17N/89.67E) at a depth of 2310 m, which utilizes the processing system GENI. The buoys were separated by a distance of 27.63 km. Wave data measured for a period of 5 months from August to December 2011, which included southwest monsoon, transition period, northeast monsoon and the passage of Thane cyclone (Fig. 2). The buoys recorded the maximum significant wave height of 3.4 m (BD02) and 3.34 m (BD08) during the passage of Thane cyclone.

The inter-comparison of wave parameters from both the buoys (IDAS and GENI) was carried out, which exhibited a good correlation of 0.96 for significant wave height (Fig. 3). The peak wave period and zero crossing wave period also are in good agreement with a correlation of 0.65 and 0.7. The lower values could be due to the local sea conditions and distance between the systems. The significant wave height (Hm0) from GENI and IDAS are also compared with Wave Watch III results, which exhibited a good correlation of 0.94 for BD08 and 0.92 for BD02 buoy.

4. Pilot Project on Wave Measurement Evaluation and Test (PP-WET)

The continuity of the established buoy networks and expansion of directional wave measurements is a priority for operational and climate assessment requirements globally. However, duration and geographical coverage of wave measurements are very limited. Apart from this, the available data need to be standardized against a reference measurement. In order to address these issues, experts in wave measurement and buoy networks had an in-depth discussion at the JCOMM (Joint WMO-IOC technical Commission for Oceanography and Marine Meteorology) Technical Workshop on Wave Measurements from Buoys (October 2008, New York, USA). The participants initiated a pilot project, PP-WET (Pilot Project on Wave Measurement Evaluation and Test), in order to develop procedures and protocols for the continuous testing and evaluation of wave measurements. The PP-WET is supported by JCOMM and leading Agencies such as Environment Canada, European Services, Marine Observation Program, NOAA (Fig. 4).

NIOT being the major service provider for moored buoy network in Indian Seas, participated in PP-WET with an objective to establish the validity of moored buoy wave measurements against the reference standard Datawell Wave Rider buoy and to build confidence in the global community (Fig. 5).

5. Wave characteristics in North Indian Ocean

Considering the long coastline along the east and west coast of India along with islands, the wave information and its variability has direct impact on various spectrums of science, technology and society. The waves in Arabian Sea (AS) and Bay of Bengal (BoB) in general exhibit significant seasonal variability in line with changing wind pattern (Fig. 6).

The dominance of southwest monsoon is well reflected with strong waves during southwest monsoon season in both AS and BoB with comparatively calm sea state for rest of the year, except during cyclone passage. The significant wave height reaches a maximum of more than 5m during southwest monsoon and remains less than 2m for rest of the period. The average wave period ranges between 6 to 8 s during southwest monsoon. The wave period lies mostly between 4 to 6 s for the remaining period, with intermittent higher wave period indicating the significant contribution from swells. The major wave direction in open ocean remains

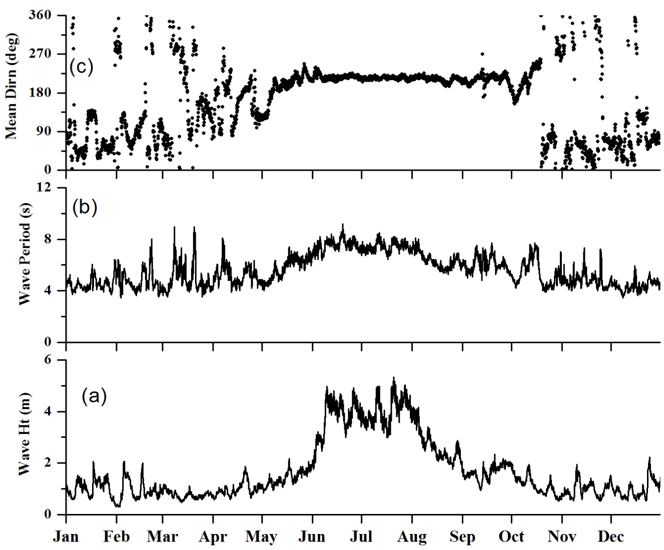

Figure 6: Time series of wave parameters in northern AS (a) - significant wave height, (b) - average wave period and (c) - mean wave direction.

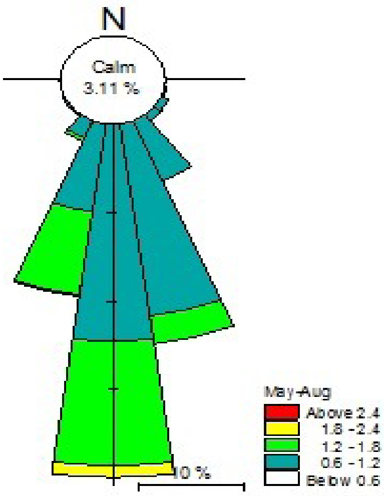

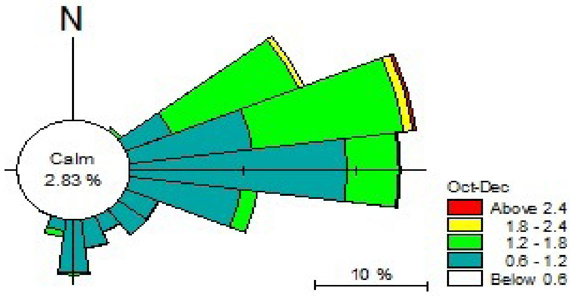

Figure 7: Rose diagram of wave height Vs. Wave direction during (a) SW monsoon and (b) NE monsoon in coastal waters of Bay of Bengal.

southwesterly for most part of the year. However, the mean wave direction changes remarkably during the northeast monsoon season. The limited northward extent restricts the propagation of waves further north and hence the southern Indian Ocean remains the major source of swell waves in AS and BoB.

Accurate wave information is vital for all types of coastal applications, design of offshore structures, effective vessel traffic management, sailing notifications, port operations and address ocean-state in general. The significant seasonal variability in wave height and mean wave direction in coastal waters of BoB are exhibited in Figure 7. The dominant wave direction is southerly with wave height less than 2.4 m, which indicates the relatively calm conditions during southwest monsoon season. The mean wave direction shifts to east-northeasterly with the presence of stronger waves exceeding 2.4 m during northeast monsoon season. The spatio temporal variability and wave transformation from deep to coastal waters remain decisive parameters in many coastal projects. The accurate modeling of wave process in coastal waters is yet to be achieved, which highlights the importance of wave measurements.

6. Summary

Systematic wave measurements are carried out by the moored buoy network maintained by NIOT since 1997. The time series of wave parameters along with the directional wave spectra provided new insight into the wave climate surrounding the Indian subcontinent, specifically in the open ocean. The significant contribution of swell waves, its origin, variability and impact on coastal dynamics are revealed by moored buoy observations. The moored buoy with indigenous wave processing software exhibited a very good correlation with imported system, established the reliability and is presently integrated in indigenous buoys. The inter comparison of NIOT wave measurements with standard Datawell Wave Rider buoy exhibited very good correlation which provided recognition among the global community.

References

1. Venkatesan, R. et al. 2013.

2. Stephen F. Barstow et al. 1984.

3. NDBC Technical Document, 1996

The North Atlantic Subpolar Gyre and Short Term Climate Predictability of Shelf Seas

Student Article

Vimal Koul[a, b]
and Johanna Baehr[a,]
[a] Institute of Oceanography, Universität Hamburg
[b] International Max Planck Research School on Earth System Modelling

Email: vimal.koul@uni-hamburg.de

There is a great value in being able to issue short term climate forecasts. Realizing such value, recent focus of predictability studies has extended to decadal climate prediction[1]. The North Atlantic Subpolar Gyre (SPG) is a promising region in such decadal prediction studies. The SPG is a relatively cold and fresh cyclonically circulating oceanic gyre with strong currents marking its periphery (Fig. 1). Variability in the strength and shape of the SPG is an important aspect of internal climate variability. The SPG is central to Atlantic-Arctic exchanges[2], impacts marine ecosystems[3], and notably, climate models show promising results in predicting variations in the SPG several years ahead[4]. Therefore, along with the questions on causes of the SPG variability and its multi-year predictability, an equally challenging question is how do we exploit such potential predictability. Shelf seas of the Northeast Atlantic Ocean can benefit from such potential predictability provided that relevant processes are identified that mediate large scale open ocean influence on shelf variables. Shelf seas are more susceptible to climate change than the open ocean and hence there is a demand for short term climate forecasts.

The first step in this endeavor is therefore to explore the SPG dynamics in a model environment. This analysis is carried out in a model environment because in order to make predictions we need to understand model dynamics, and also long term observations are either unavailable or scarce. The strengthening and weakening of the SPG corresponds to its expansion and contraction respectively (Fig. 2 and 3). The SPG strength is defined by averaging barotropic streamfunction over the SPG domain and thus represents

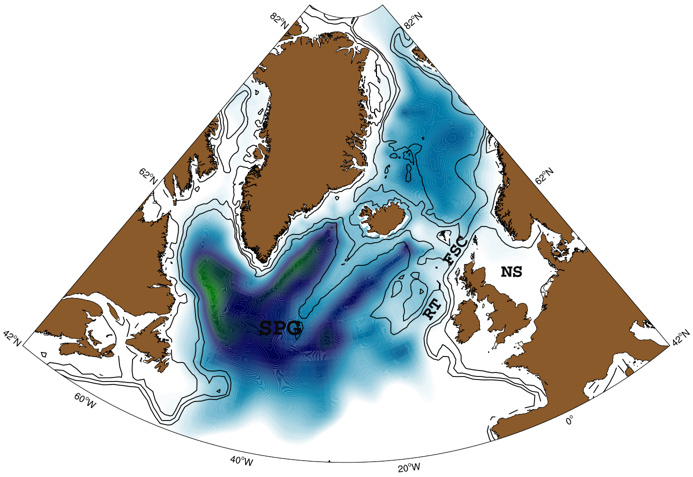

Figure 1: The subpolar gyre of the North Atlantic (SPG) in a historical (1850-2005) simulation with the coupled Max-Planck-Institute Earth System Model (MPI-ESM) in its 'low resolution' setup (MPI-ESM-LR)6. Shown is the mean barotropic streamfunction (Sv) over the entire time period; only negative values are colored. Contour lines are 200m, 1000m and 2000m isobaths. RT—Rockall Trough, FSC—Faroe-Scotland Channel and NS—North Sea.

the strength of the cyclonic circulation of the gyre. Another indicator of the SPG strength is the sea surface height, the lowering of which represents a strong gyre. Along with these two dynamically consistent indicators of the SPG strength, the SPG heat content in the model (represented in Fig. 2 as depth averaged temperature up to 645m) also follows the gyre dynamics. A weaker (and contracted) gyre is warmer that a stronger (and expanded) gyre.

The state of SPG has a profound impact on oceanic conditions of the region east of the SPG through its impact on the strength and position of the currents. The southern limit of the SPG is bounded by the North Atlantic Current (NAC) which separates subpolar water masses of the SPG to its north from water masses of the subtropical gyre to its south. However, being an extension of the Gulf Stream, the NAC predominantly carries subtropical water. When the SPG is strong, the ocean polar front (the high temperature and salinity gradient across the NAC) extends eastwards, expanding the influence of subpolar waters toward the Rockall Trough (see Fig. 1 for location). It is this subpolar influence that "dilutes" the NAC water properties throughout its journey across the North Atlantic.

The upper water masses of the North Atlantic are carried by the NAC towards the Rockall Trough from where they move to the Nordic Seas through the Faroe-Scotland Channel[5] (FSC). However, the water masses in the upper layers of the Rockall Trough have an "undiluted" subtropical origin

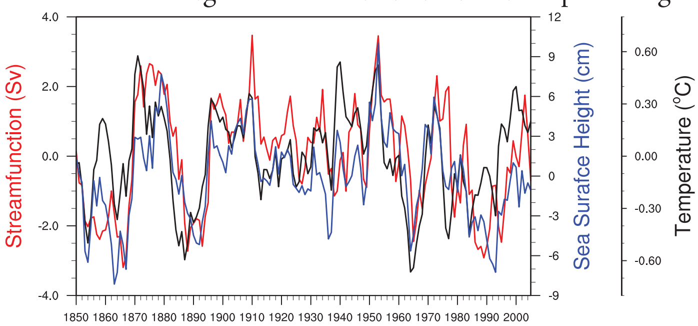

Figure 2: Time series of three SPG indices in MPI-ESM-LR using annual mean values from 1850 - 2005: (i) area averaged barotropic streamfunction (red), (ii) area averaged sea surface height (blue) (iii) area and depth (0-645m) averaged temperature (black) anomalies over 52:63°N, 26:54°W box. Anomalies are calculated with respect to 1850-2005 mean.

as well. The Eastern North Atlantic Water (ENAW), which acquires its properties west of Bay of Biscay and south of Rockall Trough fills the upper layers of the Rockall Trough. The ENAW in the Rockall Trough is warmer and more saline compared to the Western North Atlantic Water (WNAW). The WNAW is the diluted subtropical water mass, as discussed above, carried towards the Rockall region by the NAC, and is relatively fresher and colder due to the influence of subpolar water masses such as the Sub Arctic Intermediate Water (SAIW). The variability in the proportion of these water masses (ENAW and WNAW) arising from the SPG variability is contended to be the principal cause of variability in Rockall region[2].

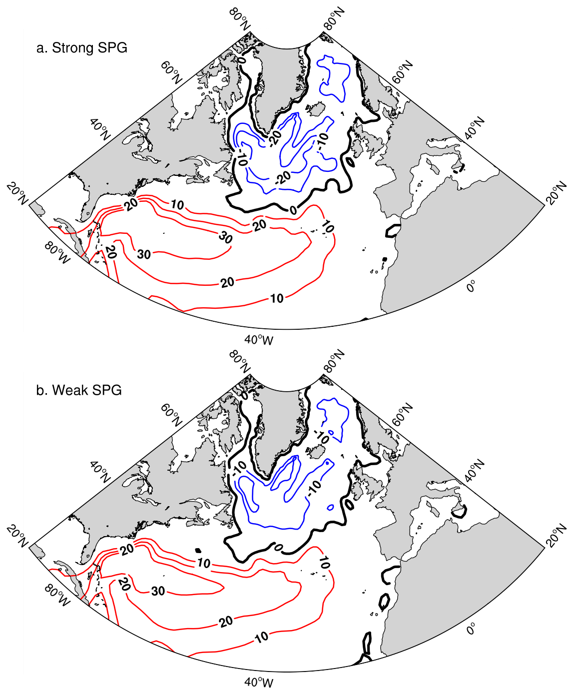

Figure 3: Composite means for a) strong SPG and b) weak SPG based on SPG index (barotropic streamfunction) values lower or higher than 1.5 standard deviations respectively. Shown are the barotropic streamfunction contours.

We hypothesize that influence of the SPG extends beyond Rockall Trough and that alternating influence of freshwater (WNAW) and saline water (ENAW) signals on FSC water properties may be predictable. Furthermore, such variations in salinity would lead to volume transport variability. The FSC is at the northern edge of North Sea, a semi-enclosed shelf sea (Fig. 1). The main inflow to North Sea, is through this channel, and between Orkney and Shetland Islands. However, the complex shelf break dynamics and the influence of winds makes it difficult to separate open ocean influence. The variation in FSC volume transport and its properties may not be the first order factor influencing on-shelf variability. It remains to be seen, if variability in the FSC (arising from the SPG) turns out to be the first order factor then there might be some hope for on-shelf decadal predictability arising from the SPG.

References

1. Marotzke, J. et al., 2016: MiKlip: A National Research Project on Decadal Climate Prediction. Bull. Amer. Meteor. Soc., 97, 2379–2394, doi: 10.1175/BAMS-D-15-00184.1.

2. Hatun, H., Sandø, A. B., Drange, H., Hansen, B.,

and Valdimarsson, H. (2005). Influence of the Atlantic subpolar gyre on the thermohaline circulation. Science, 309(5742):1841–1844.

3. Hatun, H., Lohmann, K., Matei, D., Jungclaus, J. H., Pacariz, S., Bersch, M., Gislason, A., Olafsson, J., and Reid, P. (2016). An inflated subpolar gyre blows life toward the northeastern Atlantic. Progress in Oceanography, 147:49–66.

4. Robson, J., Sutton, R., and Smith, D. (2012). Initialized decadal predictions of the rapid warming of the north Atlantic ocean in the mid 1990s. Geophysical Research Letters, 39(19).

5. Hansen, B., Østerhus, S. , Turrell, W. R., Jónsson, S. , Valdiarsson, H. , Hátún, H., and Olsen, S. M. (2008). The inflow of Atlantic water, heat, and salt to the Nordic Seas across the Greenland-Scotland Ridge, in Arctic-Subarctic Ocean Fluxes, edited by R. R. Dickson et al., pp. 15–43, Springer, Dordrecht, Netherlands.

Measuring Upper Ocean Currents from Space: Present Status and future directions/prospects

Review Article

Rajesh Sikhakolli
Atmospheric and Oceanic Sciences Group,
Space Applications Center, ISRO,
Ahmedabad

One of the important features, nature has instituted to maintain the energy balance of the earth atmosphere system is through the movement of ocean waters known as ocean currents. The variability of ocean currents happens in large range of spatio-temporal scales. The well-known "ocean conveyer belt" is the global scale thermo-haline ocean circulation mainly driven by density gradients. Whereas the upper ocean current (UOC) mainly driven by the atmospheric wind field play a very important role in redistribution of excessive heat from tropics to higher latitudes thus help in maintaining the long term balance of the earth's climate system. At interannual timescales the variability of ocean currents contributes/feedbacks to the evolution of basin scale phenomena such as Indian Ocean Dipole and El Nino events. Moreover, at regional scales they play a critical role in identifying the potential fishing zones, devising proper pollution dispersion mechanisms, mapping the oil spill trajectories and also aid in search and rescue operations. Conventionally, UOC is measured using moored as well as drifting buoys. Even though these type of observations are proved to be invaluable, this in-situ measurement strategy suffer being only available at sparse locations. On the contrary, measuring any physical parameters of ocean through satellites provides the advantage of synoptic repetitive coverage which is not possible by any other means, thus becomes a very important tool for long-term monitoring of global ocean circulation.

Even though there is no operational satellite service available for direct measurement of ocean surface currents from space, scientists have devised mechanisms to estimate this

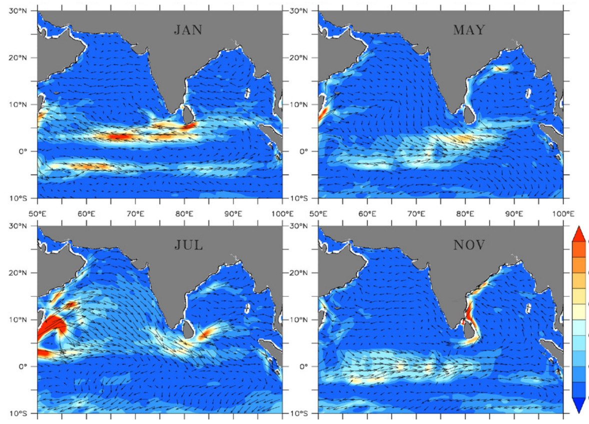

Figure 1: Monthly climatology (1993-2016) of satellite derived ocean surface currents (m/s) in the north Indian Ocean for the months of January (top left), May (top right), July (bottom left) and November (bottom right).

important variable from other satellite derived parameters. In general the absolute ocean surface current comprises of two parts based on their forcing mechanisms. The first part is the geostrophic current (Proportional to the slope of the dynamic topography) arising due to the balance between the pressure gradient force and the Coriolis force (pseudo force due to earth's rotation). Since the beginning of the era of satellite altimetry the geostrophic current is regularly mapped using altimeter derived sea surface height (SSH), (Fu., 1983, Tai., 1983). The second part is the ageostrophic or Ekman current mainly arising by the frictional force due to wind stress on the ocean surface. The satellite scatterometers which measures the ocean surface roughness, which can be used to estimate the vector winds provides to calculate the ageostrophic part of the UOC. By the synergic use of these two satellite derived parameters the absolute UOC is derived and used widely to understand the intraseasonal and interannual variability of mesoscale ocean general circulation (Lagerloef et al., 1999, Sudre et al., 2013).

However, due to equatorial singularity problem causing the non-applicability of geostrophic approximation near equator (where the Coriolis parameter tends toward zero) accuracy of these currents is not satisfactory. To overcome the problem of equatorial singularity Bonjean and Lagerloef, (2002), developed a new diagnostic model using quasi-linear and steady physics. The model formulation combines geostrophic, Ekman, and Stommel shear dynamics, and a complementary term from surface buoyancy gradient through sea surface temperature (SST) data. Since local acceleration is neglected, this diagnostic model is able to calculate the low-frequency motions in near equatorial region with improved

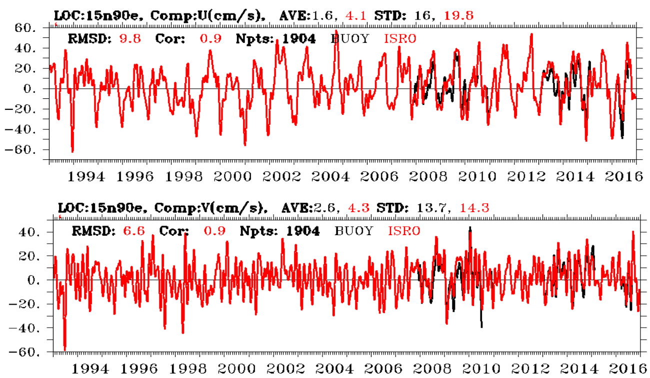

Figure 2: Time-series comparison of (a) Zonal and (b) Meridional currents of satellite derived currents (red) with RAMA buoy measured currents (black).

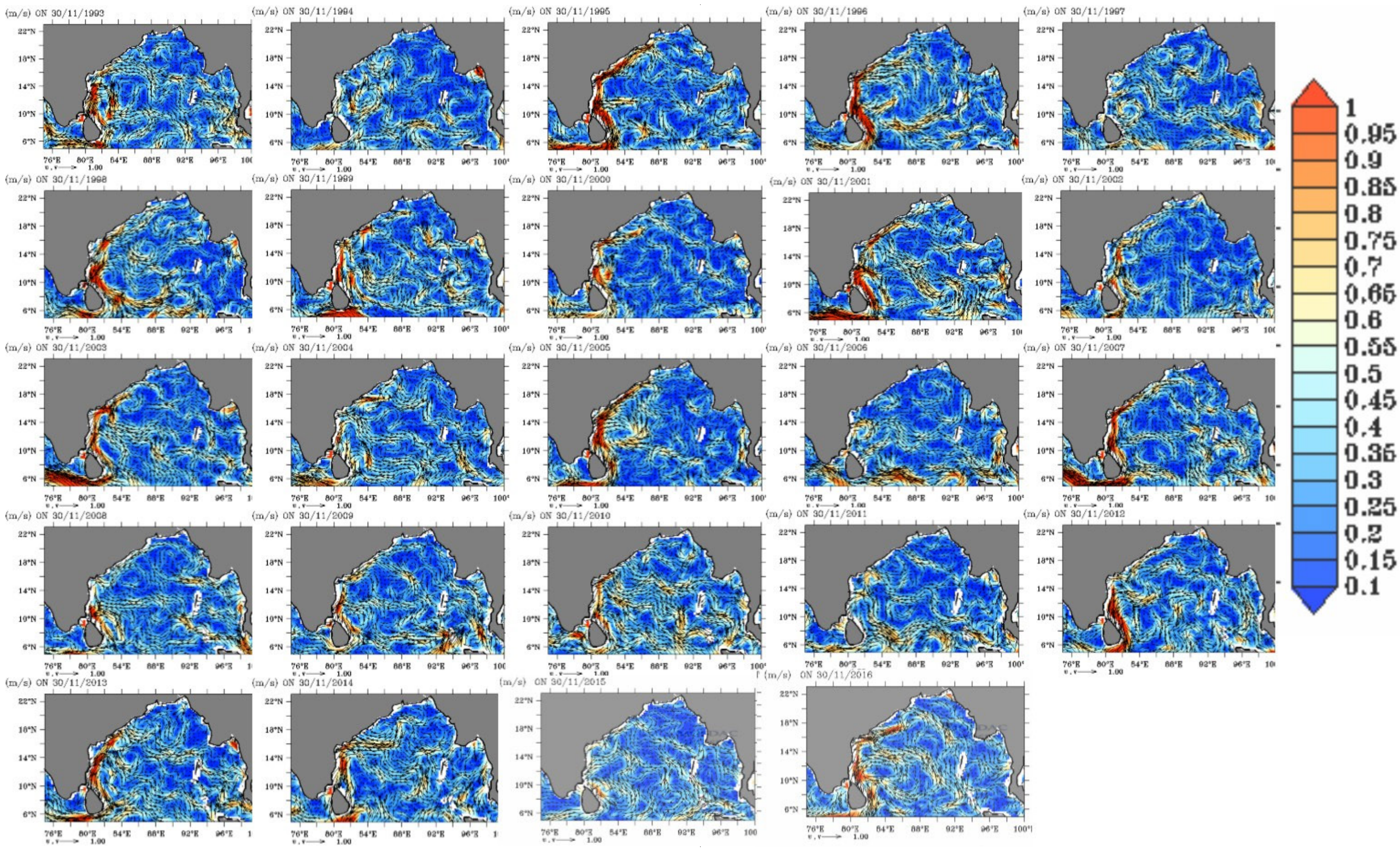

Figure 3: Ocean surface currents (m/s) in Bay of Bengal On 30th November from 1993 to 2016 depicting the interannual variability of currents. Note the East India Coastal Current (EICC) variability along East coast of India..

accuracies compared to previous studies (Sikhakolli et al., 2013a). This current product known as Ocean Surface Current Analysis Real-time (OSCAR) available at www.podaac.jpl.nasa.gov is extensively used in various process studies, understanding the current state of ocean and in evaluating the performance of Numerical Weather Prediction (NWP) models. Following similar methodology and taking advantage of the availability of high resolution gridded SSH, SST and wind data Sikhakolli et. al., (2013b) have generated a daily UOC product at 25km X 25km grid and made available to user community at www.mosdac.gov.in website. Figure 1.0 shows the monthly climatological currents during January, May, July and November for the north Indian Ocean depicting the major current systems such as East India Coastal Current (EICC), West India Coastal Current (WICC), Monsoon Current (MC), Somali Current (SC) and Equatorial Current (EC). One can observe the seasonal reversal of these currents mainly driven by the seasonally varying monsoon Winds. In figure 2.0 the time series comparison of this satellite derived currents with RAMA buoy measured currents at 15°N and 90°E in Bay of Bengal is shown conforming the high accuracy of these satellite derived currents with a root mean square error of less than 10 cm/s and a correlation coefficient of 0.9 for both zonal and meridional components. Figure 3.0 shows UOC during the month of November for Bay of Bengal from 1993 to 2016 from this satellite derived UOC dataset depicting the interannual variability of East India Coastal Current (EICC) along the East coast of India. One can clearly notice that this satellite derived current product is able to capture the weakening or absence of EICC during the IOD and El Nino years such as 1994, 1997, 2002, 2006 and 2015. Apart from this indirect way of estimating UOC from multiple satellite derived datasets there exists another, still evolving, and non-operational way to measure UOC from Synthetic Aperture Radar (SAR) measurements. Over the ocean, the SAR instrument measures surface roughness linked to, e.g., wind, waves and currents, sea ice, and surface contaminants, including natural film and oil spill. Many case studies have been demonstrated that the line-of-sight measurement of UOC is possible by measuring the phase difference among two SAR return signals from same point at two different time steps (Known as Repeat Pass Interferometry (RPI)) or at same time from two orthogonal antennas from same satellite (Known as Along Track Interferometry (ATI) (Romeiser and Thompson 2000). Few researchers have also demonstrated the use of Doppler centroid anomaly approach for measuring the line-of-sight UOC (Chapron et al 2005). Although these SAR based techniques provide high resolution (of the order of kilometers) observations of UOC, the lack global coverage, poor temporal sampling, the fact that only one component of UOC is possible to observe and the additional contribution from sources other than ocean currents, such as wind, wave etc., still limits the operational usability. In a more recent study a new mission concept by employing two chirps of opposite slope for Doppler measurement, named as "DopSCAT" is proposed by Fois et al., 2015 for simultaneous measurements of ocean surface winds and currents. Once these kind of new mission concepts are proved to be successful, the direct measurement of absolute ocean surface currents being the next remote sensing challenge seems to be achieved soon.

References

1. Lee-Lueng Fu., (1983), "Recent progress in the application of satellite altimetry to observe the mesoscale variability and general circulation of the oceans", Reviews of Geophysics and Space Physics, Vol. 21, No. 8, PP.1657-1666, November 1983.

2. Chang-Kou Tai., (1983), "On determining the large-scale ocean circulation from satellite altimetry", Jour. Geophy. Res., Vol. 88, No. C14, PP. 9553-9565, November 1983.

3. Gary S. E. Lagerloef, Gary T. Mitchum, Roger B. Lukas, and Pearn P. Niiler, (1999), "Tropical Pacific near-surface currents estimated from altimeter, wind, and drifter data", Jour. Geophy. Res., Vol. 104, No. C10, PP 23,313-23,326, October, 1999.

4. Joe¨ Sudre, Christophe Maes, and Ve´ronique Garc (2013), "On the global estimates of geostrophic and Ekman surface currents", Limnology and Oceanography: Fluids and Environments, 3 (2013): PP. 1–20, DOI 10.1215/21573689-2071927.

5. Bonjean, F., and G.S.E. Lagerloef, 2002: Diagnostic Model and Analysis of the Surface Currents in the Tropical Pacific Ocean. J. Phys. Oceanogr., 32, 2938–2954.

World of FORTRAN

Contributed Article

Manoj Kumar Tandon
Visiting Faculty
Savitribai Phule Pune University (SPPU), Pune
Symbiosis International University (SIU), Pune

Computer technology dates from an era just before the World War II i.e. from the late 1930s to the early 1940s. The second half of the twentieth century may well be called the beginning of the age of computers. Development of numerically based programming languages was taken up first in the early 1950s and FORTRAN has dominated this category since its inception. FORTRAN was the first high level computer programming language to become widely used. FORTRAN is widely used for scientific and engineering computations. It has undergone much evolution in its 50-year life. FORTRAN was designed and intended for batch processing operating and programming environment. FORTRAN is an imperative computer programming language and it supports imperative paradigms. FORTRAN is problem oriented high level programming language and its name is an acronym of FORmula TRANslation, because it was designed to allow easy translation of math formulas into computer code. FORTRAN was developed in April 1957 by a team of computer scientists at IBM for its execution on IBM-704 computer. During the initial years of FORTRAN, input for FORTRAN code was done through 80-column computer cards and 80-column FORTRAN coding form. 80-column

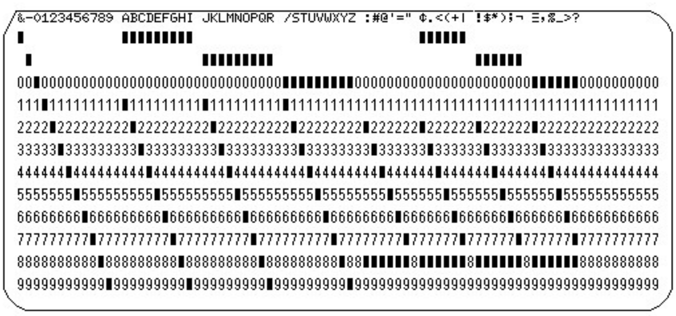

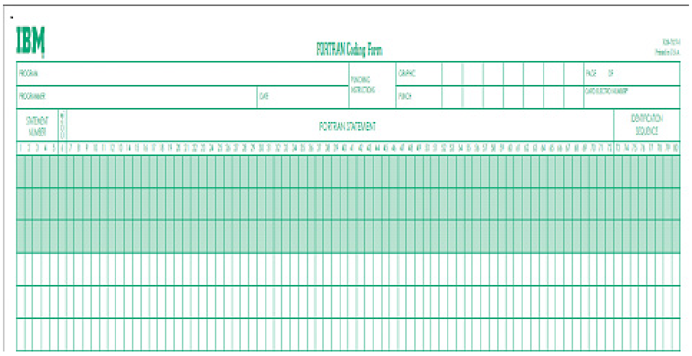

computer card is also known as 'Hollerith Card' after the name of its designer Herman Hollerith. A sample 80-column punched computer card used during the infancy days of FORTRAN for punching codes of FORTRAN programs is shown below.

John Backus was leader of the team which designed the first version of FORTRAN, a.k.a. FORTRAN-I, for the IBM-704 computer. FORTRAN-I was later revised as FORTRAN-II in 1958. FORTRAN-II was available on IBM computers such as IBM-704, IBM-1620 and others. FORTRAN-II was later on modified as FORTRAN-III in the year 1958 itself. Like FORTRAN-I, FORTRAN-III was however not released to the public. At that time, the utility of any high level programming language was open to question by programmers schooled in assembly language programming, their most serious complaint concerned the efficiency of execution of code compiled from high level language programs. As a result the design of the earliest versions of FORTRAN was oriented heavily towards providing execution efficiency. The successes of this early FORTRAN and its dependence on features oriented towards efficient execution on the IBM-704 computer have been a problem with the language. Very few at this time believed that FORTRAN could compete with hand coded assembly language; every effort was thus put into the efficient execution of FORTRAN on IBM-704. Concepts like three way arithmetic branch of FORTRAN came directly from the hardware of IBM-704. FORTRAN-III was later modified as FORTRAN-IV in the year 1961. The first standard version of FORTRAN was adopted in 1966 which lead to the emergence of FORTRAN-66 and it was released to the public in the year 1972. FORTRAN-IV was the base document for the standard version FORTRAN-66. A major revision was again made in the FORTRAN-66 standard in 1970s leading to the advent of next standard version called FORTRAN-77 which was released to the public in 1980. FORTRAN–77 continued the tradition of the original standard by allowing all data to be statically allocated. FORTRAN-77 was modified into the current standard version FORTRAN-90 which was released in 1991. The current revision of the standard, viz. FORTRAN-90 radically changed the focus of FORTRAN by allowing dynamic data. In addition, it adds the concepts of obsolescence and deprecated as indication of features that may be omitted from a future revision of FORTRAN-90, a radical departure from most standards that require compatibility with previous versions of the FORTRAN standard. The design of all versions of FORTRAN generally centers on the goal of execution efficiency. The language structures are generally simple and much of the design in inelegant, but nevertheless the goal of execution efficiency is achieved. FORTRAN-90 adds most of the modern data and control features, classically missing from FORTRAN since its inception in 1957, to give it the computing power of languages like 'C' and PASCAL. Only a restricted set of data types is provided in FORTRAN. An extensive set of operations and mathematical functions is provided in FORTRAN-90 reflecting orientation of the language towards engineering and scientific computations. Fortran-90, Fortran-95, Fortran-2003, Fortran-2008 and Fortran-2015 are the post-77 versions of FORTRAN in use at present.

Version	**Kind of Scientific Computing**
Pre-77 Fortran	Basic Computations and Control Abstractions.
Fortran-77	Structured Programming.
Fortran-90	Array Programming. Modular Programming. Generic Programming.
Fortran-95	High Performance Fortran (HPF).
Fortran-2003	Object Oriented Programming.
Fortran-2008	Concurrent Programming.
Fortran-2015	Better Interoperability between 'C' and Fortran.

The greatest weakness of FORTRAN-77 was its restricted data structuring facilities, which are essentially restricted to arrays and strings of fixed declared length. FORTRAN-77 does not have any facilities for data abstraction. Subprograms (subroutines and functions) provide the only procedural abstraction mechanism in FORTRAN-77. FORTRAN-66 was heavily influenced by the underlying computer architecture upon which it executed. FORTRAN-77 has only two levels of referencing environment viz. global and local; however FORTRAN-90 does add the concept of nested subroutines like the internal procedures of PASCAL. FORTRAN-90 has brought in the concept of dynamic variable and the phenomenon of dynamic memory management in the scientific and engineering computing domains. FORTRAN-90 has built in tools for implementing information hiding features of object oriented programming languages such as C++, JAVA and C# (pronounced as C-Sharp). FORTRAN as a programming language has amazing and astounding staying power. It was declared by many to be obsolete in 1960s, yet FORTRAN-2015 is with us today. It is a testament to FORTRAN's basic values that it continues to flourish even today. It is also the language of choice for supercomputers and high performance computers. Pre-90 versions of FORTRAN programs were based on column fixed form of coding while FORTRAN-90 introduced column free form of coding of FORTRAN programs. In column free form of coding, FORTRAN line can be as long as 132 columns. FORTRAN-90 and FORTRAN-95 allow up to 39 continuation lines whereas FORTRAN-2003 and FORTRAN-2008 allow up to 255 continuation lines. FORTRAN coding form used for writing FORTRAN codes during the earlier days of Fortran is shown below.

There are competitor languages that are considered to be superior to FORTRAN for some types of problems, but FORTRAN continues to be an excellent language for a wide variety of mathematical problems. For areas like robotics and engineering design, FORTRAN is the major language. Each revision of FORTRAN has retained the innovative pedagogical approaches of its earlier versions for ensuring compatibility and smooth transition from an earlier version to a later version. The primary objective of all the revisions of FORTRAN has been to ensure portability, reliability, maintainability and efficient execution of FORTRAN on a diverse variety of computing systems. FORTRAN is an imperative programming language supporting imperative paradigms. FORTRAN is perhaps not as popular today as it once was, but is still the programming language of choice in scientific and engineering computing environments. Individual lines of code of a FORTRAN program are easily understandable.

The overall structure of FORTRAN programs, however, tends to be rather opaque because of extensive use of statement labels and GOTOs in the control sequence mechanisms. Thus it sometimes makes it very difficult to see the overall flow of control in a FORTRAN program. Also the use of mnemonic identifiers is hampered by a restriction of six-character identifiers in the pre-90 versions of FORTRAN. The inclusion of recursive subprograms, user defined data types, user defined operators, pointers and a dynamic array in FORTRAN-90 gives FORTRAN a powerful execution model. As the language is continually evolving, some of its older limitations are becoming less important. Statement labels are no longer felt necessary in FORTRAN-90 because of the inclusion of nested multi-statement control structures. FORTRAN-90 enables its user to define his/her own data types and operators based on the computational requirements of his/her problem. FORTRAN-90 has also introduced the concept of array (dimensioned variable) of zero size in scientific and engineering computations. FORTAN-90 despite its revolutionary features and design still has a stilted look which carries over from its batch processing "80-column card deck" image. FORTRAN-90 is not just an evolutionary improvement of FORTRAN-77, it is quite different from FORTRAN-77 and has ushered a revolution in the traditional FORTRAN environment and design. Design of all versions of FORTRAN is purposely kept simple so that any user who has the knowledge of algebra up to higher secondary standard and can think logically can easily use and understand the FORTRAN language. FORTRAN-90 is a language which has salient features of programming languages such as PASCAL, 'C' and C++. Its use is no more restricted to scientific and engineering computing, but can be used in applications ranging from linguistic analysis to image processing with both qualitative and quantitative results. FORTRAN-90 can become a good tool for professional software engineering practitioners as it has all features, concepts and facilities relevant to software engineering. FORTRAN-90 can be used for "programming in the small" and "programming in the large". Unfortunately, FORTRAN-90 is a reasonably large sized programming language. FORTRAN-90 contains an elegant and powerful core language that is intellectually and educationally very appealing. Maintaining consistency with the current philosophy in language design, FORTRAN-90 has introduced the concept of slices in its dimensioned variables (arrays). A FORTRAN user has lyrically described FORTRAN as under.

"Computers are alive with sound of FORTRAN
They add and subtract with sound of FORTRAN
My code will be blessed with sound of FORTRAN

And I have to code in only FORTRAN"

PL/I was one of the earliest languages to implement slices of arrays. Like some object oriented programming languages, such as C++, FORTRAN-90 also provides the mechanism for the overloading of its subprograms and operators via INTERFACE block there by introducing the concept of polymorphism in scientific computing. Subprograms form the only abstraction mechanism in FORTRAN-77, although FORTRAN-90 does add MODULE and data types. MODULE shall be replacing COMMON blocks of pre-90 versions of FORTRAN from FORTRAN-2003 onwards. The development of FORTRAN-90 standard has been a long procedure involving several hundred people spread in many countries. FORTRAN-90 represents a rebirth of the FORTRAN computer programming language with modern features which enabled computer scientists to embed parallel computing capabilities in Fortran-2008 using Co-Arrays. High Performance FORTRAN (HPF) – dialect of Fortran-90 is specially designed to accomplish Fortran enabled High Performance Computing. If you have not been banished to computing oblivion, then you must have observed astonishing awe inspiring evolution and growth of FORTRAN since its inception in 1950s. Impressive growth of FORTRAN in tune with the ever changing domain requirements of scientific computing has flabbergasted its critics and won critical acclaims of its devoted and dedicated users. With the availability of wide range of state of the art features of scientific computing in post-77 versions of FORTRAN, scientists can now personalize scientific computing.

News and Views

Recent Updates

Teleconnection between the tropical Pacific and Antarctica

In April 2016, a large-scale breakup of land-fast ice was observed in Lutzow-Holm Bay near Syowa Station, a Japanese research facility. It was the first comparably large calving in the region since 1998. Land-fast ice is sea ice that grows along the Antarctic coast and does not move much once formed. Syowa Station is normally surrounded by land-fast ice, which makes it very difficult for even an icebreaker to reach.
According to Aoki's research, breakup latitudes in April exhibited a degree of correlation with ground-level atmospheric pressures and other indices of climate modes in

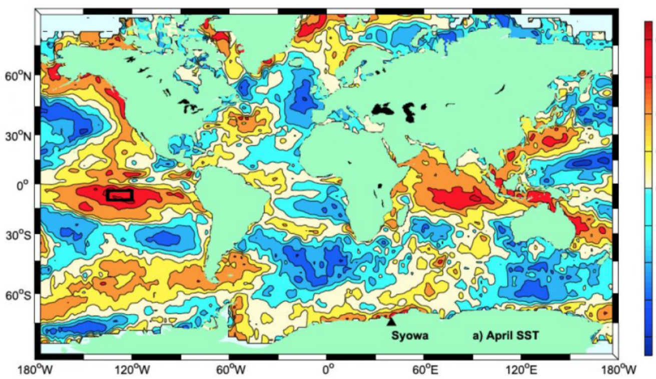

Figure 1: Map showing correlation values between the latitude of the land-fast sea ice edge in Lützow-Holm Bay and April SST.

the region. In particular, breakup latitudes highly correlated with seawater surface temperatures off Syowa Station and the tropical Pacific as far as 17,000 km away, indicating land-fast ice breakup is more often observed when seawater temperatures in the tropical Pacific are high. [Read More]

Reference: S. Aoki. Breakup of land-fast sea ice in Lützow-Holm Bay, East Antarctica, and its teleconnection to tropical Pacific sea surface temperatures. *Geophysical Research Letters*, 2017; 44 (7): 3219 DOI: 10.1002/2017GL072835.

Sea-level rise is much larger than previously thought, says study

"The sea-level acceleration over the past century has been greater than estimated by others," lead writer Eric Morrow said in a statement. Research group headed by him showed that the acceleration into the last two decades is far worse than previously thought. This new acceleration is about 25 percent higher than previous estimates.

Reference: Hay, C. C., E. Morrow, R. E. Kopp, and J. X. Mitrovica (2015), Probabilistic reanalysis of twentieth-century sea-level rise, *Nature*, 517(7535), 481–484.

Figuring out how fast Greenland is melting

A new analysis of Greenland's past temperatures will help determine how fast the island's vast ice sheet is melting. Other research shows the accelerated melting of Greenland's ice sheet is contributing to sea level rise. This new study provides the most accurate estimates of Greenland's 20th century temperatures by combining the best two of previous analyses. The finding will help improve climate models so they more accurately project future global climate change and its effects.

Reference: J. E. Jack Reeves Eyre, Xubin Zeng. Evaluation of Greenland near surface air temperature datasets. *The Cryosphere*, 2017; 11 (4): 1591 DOI:10.5194/tc-11-1591-2017.

Concurrent hot and dry summers more common in future

A combination of severe drought and a heatwave caused problems for Russia in the summer of 2010. Moscow was shrouded in thick smog, causing many deaths in the local population. At the same time, Pakistan was engulfed in heavy rain, as the high-pressure area over Russia blocked a low-pressure zone over Pakistan. This led to the country's worst flooding for centuries.

Reference: Zscheischler J, Seneviratne S. Dependence of drivers affects risks associated with compound events. *Science Advances*, 2017; 3:e1700263 DOI: 10.1126/sciadv.1700263.

Improved representation of solar variability in climate models

An international research team led by the GEOMAR Helmholtz Centre for Ocean Research Kiel and the Instituto de Astrofísica de Andalucía (CSIC) in Granada (Spain) have now published a new dataset, which will be used as a basis for all upcoming model intercomparison studies and in particular the next climate assessment report of the Intergovernmental Panel on Climate Change (IPCC). A significantly enhanced influence of solar cycle effects is expected, particularly in the stratosphere.

Reference: Katja Matthes et al., Solar forcing for CMIP6 (v3.2). Geoscientific Model Development, 2017; 10 (6):

2247 DOI: 10.5194/gmd-10-2247-2017.

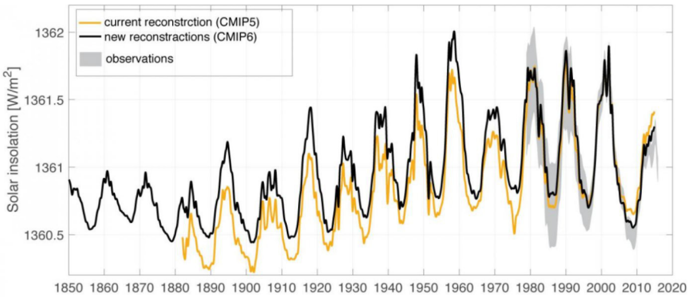

Figure 2: The yellow line shows old reconstruction, the black shows new reconstruction and the grey shaded shows observations of Solar insolation. Source: GEOMAR.

Conferences

Upcoming Events

- OSICON 2017, the 5th National Conference of the Ocean Society of India, will be held at ESSO-NCESS, Thiruvananthapuram, during 28-30 Aug 2017 [link].

- IV International Conference on El Niño Southern Oscillation: ENSO in a warmer Climate 16-18 October 2018. Guayaquil, Ecuador. Key Dates: 15 July 2017 (Call for abstracts), 31 January 2018 (Call for selected papers). 30 April 2018 (abstract submission), 15 September 2018 (full manuscript submission). For more information: http://www.ensoconference2018.org/.

- Planetary Boundary Layers in Atmospheres, Oceans, and Ice on Earth and Moons 02 Apr 2018 - 22 Jun 2018, Kavli Institute for Theoretical Physics, Santa Bar, United States. For more information: https://www.kitp.ucsb.edu/activities/blayers18.

Opportunities

Fellowships

- PhD at The International Max Planck Research School on Earth System Modelling (IMPRS-ESM), located in Hamburg, Germany. For more information, email to: office.imprs@mpimet.mpg.de.

- Postdoctoral Research Associate in Quantitative Ocean Biogeochemistry: Arise Project - Grade 7. For more information: http://www.earthworks-jobs.com/marine/liverpool17061.html

Send your correspondence and contributions to:

OSI Pune, Indian Institute of Tropical Meteorology, Pashan, Pune 411008, India.

seelan@tropmet.res.in

www.oceansociety.in/oceandigest/

Crossword

The clues for the Earth Science Crossword can be traced to the present and previous issues of Ocean Digest. Enjoy.

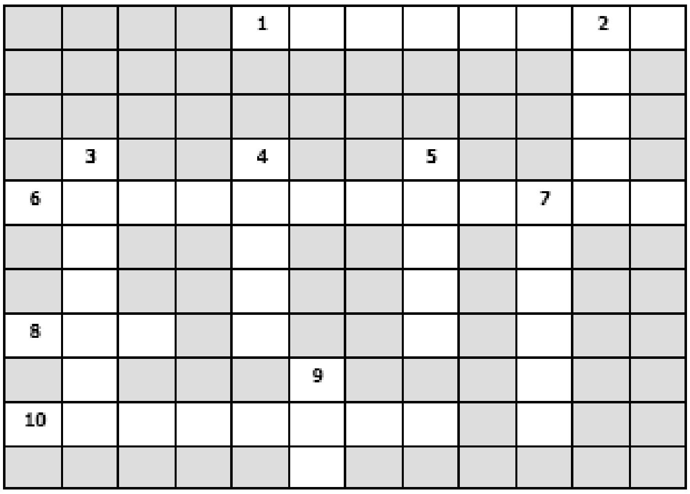

ACROSS

1. This is the highest navigable lake above the mean sea level (8)

6. These vents are formed at locations where seawater meets magma (12)

8. Visible cloud water droplets or ice crystals suspended in the air at or near the Earth's surface is better known as (3)

10. A typical name for the wind which is blowing from west to east (8)

DOWN

2. The country which is overall the highest emitter of CO_2 at the present (5)

3. A large scale air mass that rotates around a strong center of low atmospheric pressure (7)

4. The major mountain range in western North America which stretches more than 3,000 miles (5)

5. The planet with strong greenhouse effect, whose surface temperature averages 460°C (5)

7. An optical illusion caused by the refraction of light (6)

9. It is the unit of energy in CGS system of units (3).

Compiled by Bhupendra B. Singh